Event-triggered policy for dynamic output stabilization of discrete-time LPV systems under input constraints

Carla de Souza, Valter J.S. Leite, Sophie Tarbouriech, Eugênio Castelan

Event-triggered Policy for Dynamic Output Stabilization of Discrete-time LPV Systems under Input Constraints⋆

Carla de Souza[a,c,*], Valter J. S. Leite[b], Sophie Tarbouriech[c] and Eugênio B. Castelan[a]

[a]*Department of Automation and Systems Engineering, DAS/CTC/UFSC,* 88040-900*, Florianópolis, SC, Brazil.*
[b]*Department of Mechatronics Engineering, CEFET–MG, R. Álvares Azevedo, 400,* 35503-822*, Divinópolis, MG, Brazil.*
[c]*LAAS-CNRS, Université de Toulouse, CNRS, Toulouse, France.*

ABSTRACT

This paper concerns the event-triggered dynamic output-feedback control of discrete-time linear parameter-varying (LPV) systems subject to saturating actuators. Two independent event-triggering schemes are introduced to determine whether the current signals should be transmitted *a)* from the sensor to the controller and *b)* from the controller to the actuator. As a result, the communication resources can be significantly saved. Both the emulation-based problem and the co-design problem are addressed. Sufficient conditions based on linear matrix inequalities (LMIs) are derived to ensure the regional asymptotic stability of the origin for the closed-loop system. A convex optimization procedure is proposed to determine the controller matrices and the event-triggering parameters aiming at reducing the number of updates on the independent channels sensor-to-controller and controller-to-actuator. At last, numerical examples are employed to testify to the validity of the proposed methods.

1. Introduction

In the last two decades, an extensive research effort has been devoted to network control systems (NCS). These systems are characterized by the interconnection among control systems devices through a communication network. Several advantages arise from its use, such as lower costs, ease of deployment and maintenance, flexibility (see, for example, [14] and references therein). However, the communication resources of the network are often limited, which motivate new challenges in the control of systems. In this context, event-triggered control (ETC) emerged as an alternative to traditional sampled-data control [26]. The idea of the ETC is to execute control tasks after the occurrence of an event, generated by a specified event-triggering mechanism (ETM), rather than the elapse of a certain period of time, as in most traditional digital control setups. In such a way, ETC is able to significantly reduce the number of communications between process and controller, and controller and actuator, while maintaining a satisfactory closed-loop performance. The existing approaches for the design of event-triggered controllers can be issued either from emulation-based approach [7, 13] or from co-design approach [21, 29, 1]. In the emulation-based framework, only the controller or the ETC is designed while the other part is given, whereas in the co-design framework both are simultaneously designed. Although, several event-triggering schemes and control strategies have been proposed in literature (see, for example, [12, 35, 22, 33, 37, 19, 27, 36, 18, 8]), only a few explore the characteristics of the discrete-time linear parameter-varying (LPV) systems subject to input saturation.

The framework of the NCS considered in this paper is illustrated in Figure 1, where the process to be controlled is a LPV system with a saturating actuator.

To reduce the number of the sensor and the controller data transmissions in the network while preserving the stability and some certain control performance, two event generators are introduced, one in the channel between the sensor and the controller and another in the channel between the controller and the actuator. Event-triggering conditions are embedded in the event generators to determine whether the current signals (output and input) should be transmitted through the networks at every instant. As a result, the usage of the communication resources can be significantly saved.

In order to study the event-triggering scheme depicted in Figure 1, both the plant and the controller are supposed to be LPV. In the literature, some results regarding the event-triggered control for LPV systems without saturating inputs can be found. [17] addresses the co-design problem of event generator and state-feedback controller for discrete-time LPV systems where only estimated parameters satisfying certain uncertainty level is known. An event-triggered $\mathcal{H}_\infty$ control for discrete-time LPV systems is proposed in [16] by jointly designing a mixed ETM and a state feedback controller. [2] investigates the problem of discretization and digital state/output feedback control design for continuous-time LPV systems subject to a time-varying networked-induced delay. [9, 10] address an event-based reference tracking control for discrete-time LPV systems by simultaneously designing event-triggering conditions and a state feedback controller. A co-design condition in a sense of input-to-state practically stable (ISpS) of a mixed ETM and a static output-feedback controller is established in [34] for stabilization of

⋆This work has been supported by the Brazilian Agencies CAPES under the project Print CAPES-UFSC "Automation 4.0", CNPq (311208/2019-3 and 306927/2017-9); and by ANR under the project HANDY number 18-CE40-0010.

*Corresponding author

carla.souza93@hotmail.com (C. de Souza); valter@ieee.org (V.J.S. Leite); tarbour@laas.fr (S. Tarbouriech); eugenio.castelan@ufsc.br (E.B. Castelan)

ORCID(s): 0000-0002-9790-7877 (C. de Souza); 0000-0002-8177-4547 (V.J.S. Leite); 0000-0002-0816-5614 (S. Tarbouriech); 0000-0002-8079-3738 (E.B. Castelan)

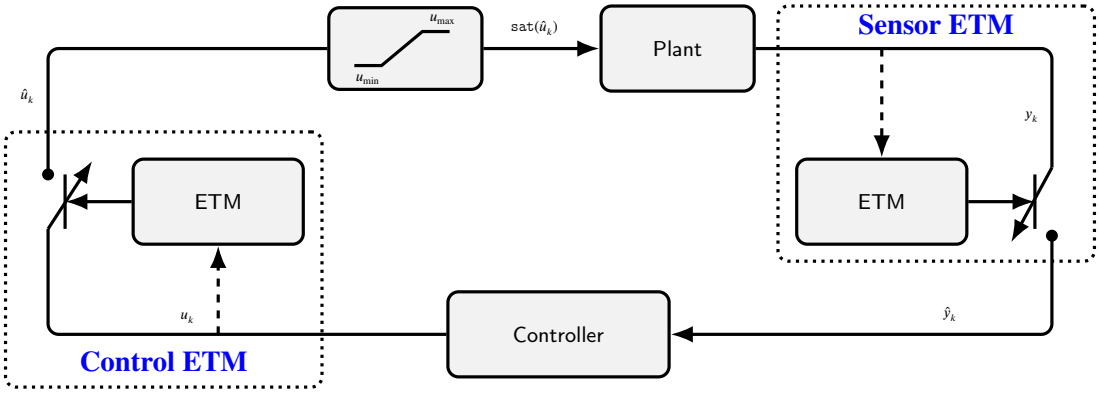

Figure 1: Event-triggering closed-loop system.

discrete-time LPV systems.

Similarly, some results considering the event-triggering control for systems subject to saturating inputs but outside the LPV paradigm have been published. [33] proposes a procedure to design a static state feedback that maximizes an estimate of the domain of attraction of saturated discrete-time system for a given triggering function. A cone complementary linearization algorithm is proposed in [38] for solving the non-convex optimization problem in order to obtain the co-design of a state-feedback controller with saturation. [11, 6] address the co-design problem for an event-triggered controller based on a static state feedback for a discrete-time system subject to actuator saturation. Also, the co-design based on a dynamic state-feedback controller is proposed in [6].

In the current paper, we address the problem depicted in Figure 1 by expanding the results obtained in [4] and [5], in which only an ETM affected the output signal. We consider an approach based on Lyapunov theory as in [26, 29, 11, 20]. Although the proposed ETM is simpler than that one studied in [25], the contribution of the current paper includes the co-design, which expects to lead to lower transmission rates. Thus, for both emulation and co-design cases, convex optimization procedures are formulated to design *a)* the output and control event generator parameters and *b)* the parameter-dependent dynamic output-feedback controller. In all cases, the objective is to reduce data transmission on the sensor-to-controller and controller-to-actuator channels. We ensure the regional asymptotic stability of the closed-loop system and characterize an estimate of the respective basin of attraction of the origin.

This paper is organized as follows. Section 2 introduces the class of systems under consideration, and states the problem to be solved. Some preliminaries results useful in the development of the conditions are given in Section 3. Section 4 presents the conditions of emulation, while Section 5 presents those of the co-design. In Section 6 are proposed optimization procedures with different control objectives. Numerical examples are given in Section 7, which verify the effectiveness of the presented approach. Finally, some concluding remarks end the paper.

Notation: $\mathbb{R}$, and $\mathbb{R}^+$ represent the set of real and non-negative real numbers, respectively. The matrix $\mathbf{0}$ stands for the null matrix of appropriate dimensions and $\mathbf{I}_n$ corresponds to the identity matrix with dimensions $n \times n$. $\mathbb{R}^{n_u \times n}$ is the set of matrices with real entries and dimensions $m \times n$. $A = \mathtt{diag}\{A_1, A_2\}$ denotes the block-diagonal matrix composed by the blocks A_1 and A_2. $A_{(\ell)}$ indicates the ℓ^{th} line of a vector or a matrix A. $\mathcal{I}[a, b]$ denotes the set of integer numbers belonging to the interval from $a \in \mathbb{N}$ to $b \in \mathbb{N}$, $b \geq a$. The symbol $\star$ represents the symmetric blocks within a matrix, $\bullet$ represents an element that has no influence on development. For $x \in \mathbb{R}^n$, $\|x\| = \sqrt{x^\top x}$ denotes the Euclidean norm and $\|x\|_Q^2$ is defined by $x^\top Q x$ with $\mathbf{0} < Q = Q^\top \in \mathbb{R}^{n \times n}$.

2. Problem Statement

The plant is described by the following model:

$$\begin{aligned} x_{p,k+1} &= A(\theta_k)x_{p,k} + B(\theta_k)\mathtt{sat}(\hat{u}_k), \\ y_k &= Cx_{p,k}, \end{aligned} \tag{1}$$

where $x_{p,k} \in \mathbb{R}^n$ is the state vector, $\hat{u}_k \in \mathbb{R}^{n_u}$ is the most recently transmitted value of the control input $u_k \in \mathbb{R}^{n_u}$, and $y_k \in \mathbb{R}^{n_y}$ is the measurable output. The symmetric saturation function, $\mathtt{sat}(\hat{u}_k)$, is given by

$$\mathtt{sat}(\hat{u}_{k(\ell)}) = \mathtt{sign}(\hat{u}_{k(\ell)}) \min(|\hat{u}_{k(\ell)}|, \bar{u}_{(\ell)}), \tag{2}$$

with $\bar{u}_{(\ell)} > 0$, $\ell \in \mathcal{I}[1, n_u]$, the limit of the saturation. The vector of time-varying parameters θ_k, which are assumed measurable and available on-line [3], lies in the unitary simplex defined by

$$\Theta \triangleq \left\{ \sum_{i=1}^{N} \theta_{k(i)} = 1,\ \theta_{k(i)} \geq 0,\ i \in \mathcal{I}[1, N] \right\}. \tag{3}$$

The matrices $A(\theta_k) \in \mathbb{R}^{n \times n}$ and $B(\theta_k) \in \mathbb{R}^{n \times n_u}$ belong to a polytopic set given by the convex combination of N known vertices as follows

$$\begin{bmatrix} A(\theta_k) & B(\theta_k) \end{bmatrix} = \sum_{i=1}^{N} \theta_{k(i)} \begin{bmatrix} A_i & B_i \end{bmatrix},\ \theta_k \in \Theta. \tag{4}$$

Remark 1. *In this paper, the system (1) can be regarded as an LPV discrete-time model issued from an identification process [31] or as a discretized version of the following continuous-time process*

$$\begin{aligned} \dot{x}_p(t) &= \tilde{A}(\theta(t))x_p(t) + \tilde{B}(\theta(t))\mathtt{sat}(u(t)), \\ y(t) &= \tilde{C}x_p(t). \end{aligned} \tag{5}$$

Note that there are several methods of discretization in the literature. One of them consists of discretizing the LPV system (5) in the same way as for LTI systems, under the assumption of slow parameter variation. In such a case, the matrices $A(\theta_k)$, $B(\theta_k)$ and C are given by the approximations $A(\theta_k) = e^{\tilde{A}(\theta(t))T_s}$, $B(\theta_k) = \int_0^{T_s} e^{\tilde{A}(\theta(t))\tau} d\tau \tilde{B}(\theta(t))$, and $C = \tilde{C}$, where T_s denotes the sampling period and $\theta_k = \theta_{kT_s} \in \Theta$, $\forall t \in [kT_s, (k+1)T_s)$ [23, 30]. In this sense, we assume the plant is controlled in a periodic event-triggering way [12, 32]. Also, the measurement is made periodically with the time interval T_s at the sampling instants and the control input is updated employing a zero-order-older (ZOH). Therefore, the approach proposed can be used to treat both continuous-time and discrete-time systems. It is also worth noting that, using this approach, the challenging problem of the minimum inter-event time for event-triggered output feedback control is overcome, since the inter-event time are at least lower bounded by the sampling period.

To stabilize the system (1), we adopt the following parameter-dependent dynamic output-feedback controller:

$$\begin{aligned} x_{c,k+1} &= A_c(\theta_k)x_{c,k} + B_c(\theta_k)\hat{y}_k - E_c(\theta_k)\Psi(\hat{u}_k), \\ u_k &= C_c(\theta_k)x_{c,k} + D_c(\theta_k)\hat{y}_k, \end{aligned} \tag{6}$$

where $x_{c,k} \in \mathbb{R}^n$ is the control state, $\Psi(\hat{u}_k) : \mathbb{R}^{n_u} \to \mathbb{R}^{n_u}$ is the dead-zone non-linearity defined by $\Psi(\hat{u}_k) = \hat{u}_k - \mathtt{sat}(\hat{u}_k)$, and $\hat{y}_k$ is the most recently transmitted value of the output measurement y_k to the controller. The anti-windup action, represented by the matrix $E_c(\theta_k) \in \mathbb{R}^{n \times n_u}$, is added to mitigate the effects caused by the saturating actuators [28]. Therefore, it acts only when the saturation occurs, i.e., wherever $\Psi(\hat{u}_k) \neq \mathbf{0}$. About the controller matrices, let us consider the following assumption:

Assumption 1. *The matrices of the controller (6) are supposed to have the following structure:*

$$\begin{bmatrix} A_c(\theta_k) & B_c(\theta_k) \end{bmatrix} = \sum_{i=1}^{N}\sum_{j=i}^{N}(1+\nu_{ij})\theta_{k(i)}\theta_{k(j)}\begin{bmatrix} \frac{A_{cij}}{2} & \frac{B_{cij}}{2} \end{bmatrix},$$

$$\begin{bmatrix} C_c(\theta_k) & D_c(\theta_k) \end{bmatrix} = \sum_{i=1}^{N}\theta_{k(i)}\begin{bmatrix} C_{ci} & D_{ci} \end{bmatrix}, E_c(\theta_k) = \sum_{i=1}^{N}\theta_{k(i)}E_{ci},$$

with $\theta_k \in \Theta$ and $\nu_{ij} = 1$ if $i \neq j$ and $\nu_{ij} = 0$ otherwise.

The controller structure introduced by Assumption 1 has a quadratic dependency on the parameter θ_k. Let us stress that any dynamic controller given in a standard polytopic form can be described according to Assumption 1 by using the fact that: $\left(\sum_{i=1}^{N}\theta_{k(i)}\right)\left(\sum_{i=1}^{N}\theta_{k(i)}M_i\right) = 0.5\sum_{i=1}^{N}\sum_{j=i}^{N}(1+\nu_{ij})\theta_{k(i)}\theta_{k(j)}M_{ij}$, with $\theta_k \in \Theta$ and $\nu_{ij} = 1$ if $i \neq j$ and $\nu_{ij} = 0$ otherwise.

However, the structure proposed in Assumption 1 is more general than the polytopic one leading to the fact that any dynamic controller satisfying Assumption 1 cannot always put in a polytopic form. Moreover, a similar but simpler development could be performed assuming $A_c(\theta)$ and $B_c(\theta)$ with polytopic description since matrices C_c and D_c do not depend on θ, i.e., they would be time-invariant.

The transmitted output $\hat{y}_k$ and the transmitted control $\hat{u}_k$ are generated by the following two independent event-triggering conditions, that shares the same clock,

$$\hat{y}_k := \begin{cases} y_k, & \|\hat{y}_{k-1} - y_k\|^2_{Q_{\Delta y}} > \|y_k\|^2_{Q_y}, \\ \hat{y}_{k-1}, & \text{otherwise}, \end{cases} \tag{7}$$

and

$$\hat{u}_k := \begin{cases} u_k, & \|\hat{u}_{k-1} - u_k\|^2_{Q_{\Delta u}} > \|u_k\|^2_{Q_u}, \\ \hat{u}_{k-1}, & \text{otherwise}, \end{cases} \tag{8}$$

where the symmetric positive definite matrices $Q_{\Delta y}$, $Q_y \in \mathbb{R}^{n_y \times n_y}$ and $Q_{\Delta u}$, $Q_u \in \mathbb{R}^{n_u \times n_u}$ are triggering parameters to be designed. These matrices act as weights on the terms associated with the triggering conditions. Their choice has a direct impact on the event-triggering policy, and, thus, on the way to reduce the data transmission. Therefore, by means of the event-triggering conditions (7) and (8), which are verified periodically, it is decided whether or not to transmit new measurements and control signals, respectively, through the network. Note that, unlike [25], the proposed mechanisms do not share the same information, which makes them independent of each other.

Due to the control input saturation, the closed loop behaves as a non-linear system, and the global stability is no longer guaranteed. In this case, the region of attraction $\mathcal{R}_{\mathcal{A}}$ in which belongs the augmented state vector $x_k = [x_{p,k}^\top \; x_{c,k}^\top]^\top \in \mathbb{R}^{2n}$, must be considered. As the exact characterization of $\mathcal{R}_{\mathcal{A}}$ is, generally, a hard task, it is important to characterize subsets with well-defined analytical representation, such as ellipsoidal and polyhedral sets. By denoting $\mathcal{R}_{\mathcal{E}}$ the estimated attraction region, then we are interested in computing $\mathcal{R}_{\mathcal{E}} \subseteq \mathcal{R}_{\mathcal{A}}$.

From this, the problems we intend to solve can be summarized as follows.

Problem 1 (Emulation problem). *Given the dynamic output feedback controller (6), which regionally stabilizes the LPV system (1) with saturating actuators in the absence of communication networks, design the two independent event-triggering conditions (7) and (8) to reduce the number of data transmissions on the sensor-to-controller and controller-to-actuator channels, respectively, while preserving the stability of the closed-loop system.*

Problem 2 (Co-design problem). *Given the LPV system (1) with saturating actuators, co-design the parameter-dependent*

dynamic output feedback controller (6) and the two independent event-triggering conditions (7) and (8), ensuring the regional asymptotic stability of the closed-loop system, while reducing the number of data transmissions on the sensor-to-controller and controller-to-actuator channels, respectively.

3. Preliminaries Results

The LPV system (1) under the dynamic controller (6), can be represented by the following model:

$$\begin{aligned} x_{k+1} &= \mathbb{A}(\theta_k)x_k - \mathbb{B}(\theta_k)\Psi(u_k) + \mathbb{E}_y(\theta_k)e_{y,k} + \mathbb{E}_u(\theta_k)e_{u,k}, \\ u_k &= \mathbb{K}(\theta_k)x_k + D_c(\theta_k)e_{y,k}, \\ y_k &= \mathbb{C}x_k, \end{aligned} \tag{9}$$

where $x_k = \begin{bmatrix} x_{p,k}^\top & x_{c,k}^\top \end{bmatrix}^\top \in \mathbb{R}^{2n}$ is the augmented state, $e_{y,k} \in \mathbb{R}^{n_y}$ is the error between the latest transmission $\hat{y}_k$ and the latest sampling y_k, and $e_{u,k} \in \mathbb{R}^{n_u}$ is the error between the latest transmission $\hat{u}_k$ and the latest sampling u_k. The parameter-varying matrices verify from Assumption 1:

$$\begin{bmatrix} \mathbb{A}(\theta_k) & \mathbb{E}_y(\theta_k) \end{bmatrix} = \sum_{i=1}^{N}\sum_{j=i}^{N}(1+\nu_{ij})\theta_{k(i)}\theta_{k(j)} \begin{bmatrix} \frac{\mathbb{A}_{ij}}{2} & \frac{\mathbb{E}_{yij}}{2} \end{bmatrix},$$

$$\begin{bmatrix} \mathbb{B}(\theta_k) & \mathbb{E}_u(\theta_k) & \mathbb{K}(\theta_k)^\top \end{bmatrix} = \sum_{i=1}^{N}\theta_{k(i)} \begin{bmatrix} \mathbb{B}_i & \mathbb{E}_{ui} & \mathbb{K}_i^\top \end{bmatrix},$$

with $\theta_k \in \Theta$ and $\nu_{ij} = 1$ if $i \neq j$ and $\nu_{ij} = 0$ otherwise, and are defined by

$$\mathbb{A}_{ij} = \begin{bmatrix} A_i + A_j + (B_i D_{cj} + B_j D_{ci})C & B_i C_{cj} + B_j C_{ci} \\ B_{cij}C & A_{cij} \end{bmatrix},$$
$$\mathbb{B}_i = \begin{bmatrix} B_i \\ E_{ci} \end{bmatrix}, \ \mathbb{E}_{ui} = \begin{bmatrix} B_i \\ \mathbf{0} \end{bmatrix}, \ \mathbb{E}_{yij} = \begin{bmatrix} B_i D_{cj} + B_j D_{ci} \\ B_{cij} \end{bmatrix},$$
$$\mathbb{K}_i = \begin{bmatrix} D_{ci}C & C_{ci} \end{bmatrix}, \text{ and } \mathbb{C} = \begin{bmatrix} C & \mathbf{0} \end{bmatrix}.$$

Note that if y_k is updated at instant k, then from (7) it follows that $e_{y,k} = \hat{y}_k - y_k = y_k - y_k = \mathbf{0}$, and if y_k is not updated at instant k, then from (7) it also follows that $e_{y,k} = \hat{y}_k - y_k = \hat{y}_{k-1} - y_k$. In other words, the following inequality is always satisfied:

$$\|e_{y,k}\|^2_{Q_{\Delta_y}} \leq \|y_k\|^2_{Q_y}. \tag{10}$$

Similarly, if u_k is updated at instant k, then from (8) one gets $e_{u,k} = u_k - u_k = \mathbf{0}$, and if u_k is not updated at instant k, then from (8) one gets $e_{u,k} = \hat{u}_{k-1} - u_k$. Consequently, the following condition always holds

$$\|e_{u,k}\|^2_{Q_{\Delta u}} \leq \|u_k\|^2_{Q_u}. \tag{11}$$

To investigate the regional asymptotic stability of the closed-loop system (9), we use the following candidate Lyapunov function

$$V(x_k) = x_k^\top P^{-1}(\theta_k)x_k, \tag{12}$$

where $P(\theta_k) = \sum_{i=1}^{N}\theta_{k(i)}P_i$, with $\mathbf{0} < P_i = P_i^\top \in \mathbb{R}^{2n\times 2n}$ and $\theta_k \in \Theta$. If (12) is a Lyapunov function, then the estimated attraction region is computed through an associated level set $\mathcal{R}_\mathcal{E} = \mathcal{L}_\mathcal{V}(1) = \{x_k \in \mathbb{R}^{2n} : V(x_k) \leq 1\}$, which can be computed as [15, Lemma 4]:

$$\mathcal{R}_\mathcal{E} = \mathcal{L}_\mathcal{V}(1) = \bigcap_{\forall\theta_k\in\Theta} \mathcal{E}(P(\theta_k)^{-1}, 1) = \bigcap_{i\in\mathcal{I}[1,N]} \mathcal{E}(P_i^{-1}, 1), \tag{13}$$

with

$$\mathcal{E}(P_i^{-1}, 1) = \left\{x_k \in \mathbb{R}^{2n} : x_k^\top P_i^{-1} x_k \leq 1\right\}. \tag{14}$$

In addition, to deal with the saturation, we use the following property directly derived from [28, Lemma 1.6, p. 43].

Lemma 1. *Let u_k given by (6), $\bar{u} \in \mathbb{R}^{n_u}_+$, and a matrix $\mathbb{G}(\theta_k) = \sum_{i=1}^{N}\theta_{k(i)}\mathbb{G}_i$ with $\mathbb{G}_i \in \mathbb{R}^{n_u\times 2n}$ for $\mathcal{I}[1,N]$ and $\theta_k \in \Theta$, such that*

$$\mathcal{S}(\bar{u}) \triangleq \{x_k \in \mathbb{R}^{2n} : |\mathbb{G}(\theta_k)x_k| \leq \bar{u}\}.$$

If $x_k \in \mathcal{S}(\bar{u})$, then for any diagonal positive definite matrix $\mathbb{T} \in \mathbb{R}^{n_u\times n_u}$, the following inequality is verified

$$\Psi(\hat{u}_k)^\top\mathbb{T}(\Psi(\hat{u}_k) - (\mathbb{K}(\theta_k) - \mathbb{G}(\theta_k))x_k - D_c(\theta_k)e_{y,k} - e_{u,k}) \leq \mathbf{0}.$$

4. Emulation-based approach

In this section, we provide a solution to Problem 1. In this case, we assume that the dynamic output-feedback controller (6), which can regionally stabilize the system (1) in the absence of communication networks, is available and we design the parameters of the event-triggering rules (7) and (8) that minimize the update rate on both channels.

Theorem 1. *Consider the LPV system (1) in closed-loop with the dynamic output-feedback controller (6), where the matrices A_{cij}, B_{cij}, C_{ci}, D_{ci}, and E_{ci} of the controller are given. Suppose that there exist symmetric positive definite matrices $P_i \in \mathbb{R}^{2n\times 2n}$, $Q_{\Delta u}$, $\hat{Q}_u \in \mathbb{R}^{n_u\times n_u}$, $Q_{\Delta y}$, $\hat{Q}_y \in \mathbb{R}^{n_y\times n_y}$, a positive definite diagonal matrix $S \in \mathbb{R}^{n_u\times n_u}$, matrices $U \in \mathbb{R}^{2n\times 2n}$ and $H_i \in \mathbb{R}^{n_u\times 2n}$, with $i \in \mathcal{I}[1,N]$ and $j \in \mathcal{I}[i,N]$, such that (15) (provided at the top of the next page) and the following LMI condition are feasible,*

$$\begin{bmatrix} U + U^\top - P_i & \star \\ H_{i(\ell)} & \bar{u}^2_{(\ell)} \end{bmatrix} > \mathbf{0}, i \in \mathcal{I}[1,N], \ell \in \mathcal{I}[1,n_u]. \tag{16}$$

Then, the closed-loop system (9) subject to the ETMs (7) and (8) with matrices $Q_{\Delta u}$, $Q_u = \hat{Q}_u^{-1}$, $Q_{\Delta y}$ and $Q_y = \hat{Q}_y^{-1}$ is regionally asymptotically stable and has a reduced number of data transmissions on the sensor-to-controller and the controller-to-actuator channels. Moreover, the region $\mathcal{R}_\mathcal{E}$, computed in (13)-(14), is an estimate of the region of attraction of the origin for the closed-loop system.

$$\left[\begin{array}{c|c|c|c|c|c|c} U+U^{\top} & \star & \star & \star & \star & \star & \star \\ -\frac{1}{2}(P_i+P_j) & & & & & & \\ \hline \mathbf{0} & Q_{\Delta u} & \star & \star & \star & \star & \star \\ \hline \mathbf{0} & \mathbf{0} & Q_{\Delta y} & \star & \star & \star & \star \\ \hline \frac{1}{2}(H_i+H_j-\mathbb{K}_iU-\mathbb{K}_jU) & -\mathbf{I}_{n_u} & -\frac{1}{2}(D_{ci}+D_{cj}) & 2S & \star & \star & \star \\ \hline \frac{1}{2}\mathbb{A}_{ij}U & \frac{1}{2}(\mathbb{E}_{uj}+\mathbb{E}_{uj}) & \frac{1}{2}\mathbb{E}_{yij} & -\frac{1}{2}(\mathbb{B}_i+\mathbb{B}_j)S & \hat{P}_r & \star & \star \\ \hline \frac{1}{2}(\mathbb{K}_i+\mathbb{K}_j)U & \mathbf{0} & \frac{1}{2}(D_{ci}+D_{cj}) & \mathbf{0} & \mathbf{0} & \hat{Q}_u & \star \\ \hline \mathbb{C}U & \mathbf{0} & \mathbf{0} & \mathbf{0} & \mathbf{0} & \mathbf{0} & \hat{Q}_y \end{array}\right] > \mathbf{0}, \tag{15}$$

$$r, i \in \mathcal{I}[1,N], j \in \mathcal{I}[i,N],$$

$$\left[\begin{array}{ccccccc} P^{-1}(\theta_k) & \star & \star & \star & \star & \star & \star \\ \mathbf{0} & Q_{\Delta u} & \star & \star & \star & \star & \star \\ \mathbf{0} & \mathbf{0} & Q_{\Delta y} & \star & \star & \star & \star \\ -S^{-1}(\mathbb{K}(\theta_k)-\mathbb{G}(\theta_k)) & -\mathbf{I}_{n_u} & -S^{-1}D_c(\theta_k) & 2S^{-1} & \star & \star & \star \\ \mathbb{A}(\theta_k) & \mathbb{E}_u(\theta_k) & \mathbb{E}_y(\theta_k) & -\mathbb{B}(\theta_k) & P(\theta_{k+1}) & \star & \star \\ \mathbb{K}(\theta_k) & \mathbf{0} & D_c(\theta_k) & \mathbf{0} & \mathbf{0} & \hat{Q}_u & \star \\ \mathbb{C} & \mathbf{0} & \mathbf{0} & \mathbf{0} & \mathbf{0} & \mathbf{0} & \hat{Q}_y \end{array}\right] > \mathbf{0}. \tag{19}$$

Proof 1. *By supposing the feasibility of (16), multiply its left-hand side by $\theta_{k(i)}$ and sum it up for $i \in \mathcal{I}[1,N]$. Then, replace $H(\theta_k)$ by $G(\theta_k)U$, use the fact that $[P(\theta_k)-U]^{\top}\times P^{-1}(\theta_k)[P(\theta_k)-U] \geq \mathbf{0}$ or equivalently $U^{\top}+U-P(\theta_k) \leq U^{\top}P^{-1}(\theta_k)U$, and pre- and post-multiply the resulting inequality by the matrix $\mathtt{diag}\{U^{-\top},1\}$, to obtain*

$$\begin{bmatrix} P^{-1}(\theta_k) & \star \\ \mathbb{G}(\theta_k)_{(\ell)} & \bar{u}^2_{(\ell)} \end{bmatrix} > \mathbf{0}. \tag{17}$$

Finally, apply Schur complement and pre- and post-multiply the resulting inequality by $x_k^{\top}$ and x_k, respectively, to obtain

$$-x_k^{\top}P(\theta_k)^{-1}x_k + x_k^{\top}\mathbb{G}(\theta_k)_{(\ell)}^{\top}(\bar{u}^2_{(\ell)})^{-1}\mathbb{G}(\theta_k)_{(\ell)}x_k \leq 0, \tag{18}$$

which ensures $V(x_k) = x_k^{\top}P^{-1}(\theta_k)x_k \leq 1$, and $|\mathbb{G}(\theta_k)x_k| \leq \bar{u}$, and consequently, $\mathcal{R}_{\mathcal{E}} \subseteq \mathcal{S}(\bar{u})$. Thus, any trajectory of the closed-loop system belonging to $\mathcal{R}_{\mathcal{E}}$ belongs also to $\mathcal{S}(\bar{u})$. Therefore, the feasibility of (16) implies that the region $\mathcal{R}_{\mathcal{E}}$ is included in $\mathcal{S}(\bar{u})$, and consequently, Lemma 1 applies.

Moreover, by supposing the feasibility of (15), we have from block (1,1) that U is non-singular. So, first multiply the left-hand side of (15) by $\theta_{k+1(r)}$, $\theta_{k(i)}$ and $\theta_{k(j)}$, and sum it up for $r,i \in \mathcal{I}[1,N]$ and $j \in \mathcal{I}[1,N]$. Then, replace $H(\theta_k)$ by $\mathbb{G}(\theta_k)U$ and use the fact that $[P(\theta_k)-U]^{\top}P^{-1}(\theta_k)[P(\theta_k)-U] \geq \mathbf{0}$ or equivalently $U^{\top}+U-P(\theta_k) \leq U^{\top}P^{-1}(\theta_k)U$. Next, pre- and post-multiply the resulting inequality by the matrix $\mathtt{diag}\{U^{-\top},\mathbf{I}_{n_u},\mathbf{I}_{n_y},S^{-1},\mathbf{I}_{2n},\mathbf{I}_{n_u},\mathbf{I}_{n_y}\}$ and its transpose, respectively, to obtain the inequality (19) (provided at the top of the next page).

After that, apply Schur complement, pre- and post-multiply the resulting inequality by the augmented vector $X_k^{\top} = \begin{bmatrix} x_k^{\top} & e_{u,k}^{\top} & e_{y,k}^{\top} & \Psi(\hat{u}_k)^{\top} \end{bmatrix}$ and X_k, respectively, and replace $\mathbb{A}(\theta_k)x_k+\mathbb{E}_u(\theta_k)e_{u,k}+\mathbb{E}_y(\theta_k)e_{y,k}-\mathbb{B}(\theta_k)\Psi(\hat{u}_k)$ by x_{k+1} according to (9), to obtain

$$\begin{aligned} x_{k+1}^{\top}P^{-1}(\theta_{k+1})x_{k+1} - x_k^{\top}P^{-1}(\theta_k)x_k - 2\Psi(\hat{u}_k)^{\top}\mathbb{T}\Big(\Psi(\hat{u}_k) \\ -(\mathbb{K}(\theta_k)-\mathbb{G}(\theta_k))x_k - D_c(\theta_k)e_{y,k} - e_{u,k}\Big) - e_{u,k}^{T}Q_{\Delta u}e_{u,k} \\ + u_k^{T}Q_u u_k - e_{y,k}^{T}Q_{\Delta y}e_{y,k} + y_k^{T}Q_y y_k \leq 0 \end{aligned} \tag{20}$$

Finally, assume that $x_{k+1}^{\top}P^{-1}(\theta_{k+1})x_{k+1} - x_k^{\top}P^{-1}(\theta_k)x_k$ is equivalent to $V(x_{k+1}) - V(x_k) = \Delta V(x_k)$, and denote $S^{-1} = \mathbb{T}$, $\hat{Q}_y^{-1} = Q_y$, and $\hat{Q}_u^{-1} = Q_u$, to get

$$\begin{aligned} \Delta V(x_k) < 2\Psi(\hat{u}_k)^{\top}\mathbb{T}\Big(\Psi(\hat{u}_k) - (\mathbb{K}(\theta_k)-\mathbb{G}(\theta_k))x_k \\ - D_c(\theta_k)e_{y,k} - e_{u,k}\Big) < e_{u,k}^{\top}Q_{\Delta u}e_{u,k} - u_k^{\top}Q_u u_k \\ + e_{y,k}^{\top}Q_{\Delta y}e_{y,k} - y_k^{\top}Q_y y_k \leq 0. \end{aligned} \tag{21}$$

Hence, the feasibility of (15) ensures the positivity of the function given in (12) and the negativity of $\Delta V(x_k)$. Also, by inequalities (10) and (11), we have that the event-triggering conditions (7) and (8) are always satisfied, respectively.

Therefore, by Lyapunov theory, the regional stability of closed-loop system (9) under the event-triggering mechanisms (7) and (8) is ensured whenever the state trajectories evolve inside the estimated attraction region $\mathcal{R}_{\mathcal{E}}$, computed as in (13)-(14), and the sensor-to-controller and controller-to-actuator channels will have a reduced data transmission rate, whenever (10) and (11) are verified.

Remark 2. *Theorem 1 can be adapted to treat particular cases usually found in the literature, in which there is an*

event generator in only one of the communication channels (see, for example, [37, 4, 5, 6]). To consider an event generator only in the channel between the sensor and the controller, it is necessary to delete the second and the sixth lines and columns of the LMI (15). On the other hand, to admit an event generator only in channel between the controller and the sensor, we have to delete the third and the seventh lines and columns of the LMI (15).

5. Co-design approach

In the previous section, the dynamic output-feedback controller is supposed to be known, and capable to regionally stabilize the system (1) without communication networks. Therefore, only the event-triggering mechanisms are designed by Theorem 1. The disadvantage is that the control performance of the closed-loop system may be constrained by the previously selected controller. To overcome such a restriction, a co-design approach of the dynamic controller and the event-triggering mechanisms is proposed in this section, thus providing a solution to Problem 2.

Let us start by introducing some matrices useful to the developments. Thus, inspired by [24], we use matrices X, Y, W and, $Z \in \mathbb{R}^{n\times n}$ to define

$$U = \begin{bmatrix} X & \bullet \\ Z & \bullet \end{bmatrix}, \quad U^{-1} = \begin{bmatrix} Y & \bullet \\ W & \bullet \end{bmatrix}, \Phi = \begin{bmatrix} Y & \mathbf{I}_n \\ W & \mathbf{0} \end{bmatrix}, \tag{22}$$

which yield

$$U\Phi = \begin{bmatrix} \mathbf{I}_n & X \\ \mathbf{0} & Z \end{bmatrix} \text{ and } \hat{U} = \Phi^\top U \Phi = \begin{bmatrix} Y^\top & M^\top \\ \mathbf{I}_n & X \end{bmatrix}, \tag{23}$$

where, by construction, we have

$$M^\top = Y^\top X + W^\top Z. \tag{24}$$

By partitioning matrix $P = \begin{bmatrix} P_{11} & \star \\ P_{21} & P_{22} \end{bmatrix}$, one obtains:

$$\hat{P}_i = \Phi^\top P_i \Phi = \begin{bmatrix} \hat{P}_{i11} & \star \\ \hat{P}_{i21} & \hat{P}_{i22} \end{bmatrix}, \tag{25}$$

with $\hat{P}_{i11} = Y^\top P_{i11} Y + W^\top P_{i12}^\top Y + Y^\top P_{i12} W + W^\top P_{i22} W$, $\hat{P}_{i21} = P_{i11}^\top Y + P_{i12} W$, and $\hat{P}_{i22} = P_{i11}$. With the aid of matrices in (22)-(25), we can provide a solution to Problem 2 through the next theorem.

Theorem 2. *Consider there exist symmetric positive definite matrices $\hat{P}_i \in \mathbb{R}^{2n\times 2n}$, $Q_{\Delta u}$, $\hat{Q}_u \in \mathbb{R}^{n_u\times n_u}$, $Q_{\Delta y}$, $\hat{Q}_y \in \mathbb{R}^{n_y\times p}$, a positive definite diagonal matrix $S \in \mathbb{R}^{n_u\times n_u}$, and matrices X, Y, M, $\hat{A}_{cij}$, $\hat{B}_{cij}$, $\hat{C}_{ci}$, $\hat{D}_{ci}$, and $\hat{E}_{ci}$ of appropriate dimensions, with $i \in \mathcal{I}[1, N]$ and $j \in \mathcal{I}[i, N]$, such that (26) (given at the top of this page) and the following LMI conditions are feasible,*

$$\begin{bmatrix} \hat{U} + \hat{U}^\top - \hat{P}_i & \star \\ H_{i(\ell)} & \bar{u}^2_{(\ell)} \end{bmatrix} > \mathbf{0}, i \in \mathcal{I}[1, N], \ell \in \mathcal{I}[1, n_u], \tag{27}$$

with

$$\Xi_{1ij} = \begin{bmatrix} (\hat{D}_{ci} + \hat{D}_{cj})C & \hat{C}_{ci} + \hat{C}_{cj} \end{bmatrix},$$
$$\Xi_{2ij} = \begin{bmatrix} Y^\top(A_i + A_j) + \hat{B}_{cij}C & \hat{A}_{cij} \\ A_i + A_j + (B_i\hat{D}_{cj} + B_j\hat{D}_{cj})C & (A_i + A_j)X + (B_i\hat{C}_{cj} + B_j\hat{C}_{ci}) \end{bmatrix},$$
$$\Xi_{3ij} = \begin{bmatrix} Y^\top(B_i + B_j) \\ B_i + B_j \end{bmatrix}, \Xi_{4ij} = \begin{bmatrix} \hat{B}_{cij} \\ B_i\hat{D}_{cj} + B_j\hat{D}_{ci} \end{bmatrix},$$
$$\Xi_{5ij} = \begin{bmatrix} -(\hat{E}_{ci} + \hat{E}_{cj}) \\ -(B_j + B_i)S \end{bmatrix}, \text{ and } \hat{U} = \begin{bmatrix} Y^\top & M^\top \\ \mathbf{I}_n & X \end{bmatrix}.$$

Then, by choosing non-singular matrices W and Z such that (24) holds, we have that the saturated LPV system (1) under the dynamic output-feedback compensator (6) with matrices defined by

$$\begin{bmatrix} A_{cij} & B_{cij} \\ C_{ci} & D_{ci} \end{bmatrix} = \begin{bmatrix} W^\top & Y^\top(B_i + B_j) \\ \mathbf{0} & \mathbf{I}_{n_u} \end{bmatrix}^{-1} \times \begin{bmatrix} \hat{A}_{cij} - Y^\top(A_i + A_j)X & \hat{B}_{cij} \\ \hat{C}_i & \hat{D}_i \end{bmatrix} \begin{bmatrix} Z & \mathbf{0} \\ CX & \mathbf{I}_{n_y} \end{bmatrix}^{-1}$$
$$E_{ci} = (W^{-1})^\top(\hat{E}_{ci}S^{-1} - Y^\top B_i), \tag{28}$$

subject to the ETMs (7) and (8) with matrices $Q_{\Delta u}$, $Q_u = \hat{Q}_u^{-1}$, $Q_{\Delta y}$ and $Q_y = \hat{Q}_y^{-1}$ is regionally asymptotically stable and has a reduced number of data transmissions on the sensor-to-controller and controller-to-actuator channels. Moreover, the region $\mathcal{R}_\mathcal{E}$, computed in (13)-(14), is an estimate of the region of attraction of the origin for the closed-loop system.

Proof 2. *By supposing the feasibility of (26), from block (1,1), we have that $\hat{U} + \hat{U}^\top > 0$, and consequently, $\hat{U}$ is non-singular. In view of (23), X and Y are also non-singular, and by rewritten $\hat{U}$ as*

$$\begin{bmatrix} Y^\top & M^\top \\ \mathbf{I}_n & X \end{bmatrix} = \begin{bmatrix} \mathbf{I}_n & Y^\top \\ \mathbf{0} & \mathbf{I}_n \end{bmatrix} \begin{bmatrix} \mathbf{0} & M^\top - Y^T X \\ \mathbf{I}_n & X \end{bmatrix}, \tag{29}$$

we can also verify the non-singularity of $(M^\top - Y^\top X)$. As a result, it is always possible to choose non-singular matrices W and Z, such that (24) is verified. This shows that the gains (28) are well-defined.

Furthermore, consider the matrices (22)-(25) and the following change of variables

$$\begin{bmatrix} \hat{A}_{cij} & \hat{B}_{cij} \\ \hat{C}_i & \hat{D}_i \end{bmatrix} = \begin{bmatrix} W^\top & Y^\top(B_i + B_j) \\ \mathbf{0} & \mathbf{I}_{n_u} \end{bmatrix} \begin{bmatrix} A_{cij} & B_{cij} \\ C_{ci} & D_{ci} \end{bmatrix} \times \begin{bmatrix} Z & \mathbf{0} \\ CX & \mathbf{I}_{n_y} \end{bmatrix} + \begin{bmatrix} Y^\top(A_i + A_j)X & \mathbf{0} \\ \mathbf{0} & \mathbf{0} \end{bmatrix},$$
$$\hat{E}_{ci} = W^\top E_{ci} S + Y^\top B_i S, \tag{30}$$

by pre- and post-multiplying (26) by $\mathtt{diag}\{\Phi^{-\top}, \mathbf{I}_{n_u}, \mathbf{I}_{n_y}, \Phi^{-\top}, \mathbf{I}_{n_u}, \mathbf{I}_{n_y}\}$ and its transpose, respectively, one gets (15). Similarly, by pre- and post-multiplying (27) by $\mathtt{diag}\{\Phi^{-\top}, 1\}$

$$\left[\begin{array}{c|c|c|c|c|c|c} \hat{U}+\hat{U}^\top - \frac{1}{2}(\hat{P}_i+\hat{P}_j) & \star & \star & \star & \star & \star & \star \\ \hline \mathbf{0} & Q_{\Delta u} & \star & \star & \star & \star & \star \\ \hline \mathbf{0} & \mathbf{0} & Q_{\Delta y} & \star & \star & \star & \star \\ \hline \frac{1}{2}(H_i+H_j-\Xi_{1ij}) & -\mathbf{I}_{n_u} & -\frac{1}{2}(\hat{D}_{ci}+\hat{D}_{cj}) & 2S & \star & \star & \star \\ \hline \frac{1}{2}\Xi_{2ij} & \frac{1}{2}\Xi_{3ij} & \frac{1}{2}\Xi_{4ij} & \frac{1}{2}\Xi_{5ij} & \hat{P}_r & \star & \star \\ \hline \frac{1}{2}\Xi_{1ij} & \mathbf{0} & \frac{1}{2}(\hat{D}_{ci}+\hat{D}_{cj}) & \mathbf{0} & \mathbf{0} & \hat{Q}_u & \star \\ \hline \begin{bmatrix} C & CX \end{bmatrix} & \mathbf{0} & \mathbf{0} & \mathbf{0} & \mathbf{0} & \mathbf{0} & \hat{Q}_y \end{array}\right] > \mathbf{0},\ r,i \in \mathcal{I}[1,N], j \in \mathcal{I}[i,N] \tag{26}$$

and its transpose, respectively, one obtains (16). Thus, as in the proof of Theorem 1, these two equivalences allow to conclude the proof.

Remark 3. *The design of the dynamic controller (7) through (26) in Theorem 2 imposes, for given X, Y and M, to compute non-singular matrices W and Z satisfying (24) or, equivalently, $W^\top Z = M^\top - Y^\top X$. However, the choice of these matrices can be performed in different ways, for example, we can set $W = \gamma \mathbf{I}$, for any given scalar γ, and compute $Z = (M^\top - Y^\top X)\gamma^{-1}$, or even use any matrix decomposition, such as LU and QR factorizations, to determine them.*

Remark 4. *Theorems 1 and 2 can be simplified to deal with LTI and non-saturated systems. In the LTI case, it is required to set $r = i = j = 1$, which results in fixed matrices. Notice that, the dynamic and input matrices of the controller, A_c and B_c, are retrieved by setting $A_{c11} = 0.5A_{c11}$ and $B_c = 0.5B_{c11}$, according to Assumption 1, with A_{c11} and B_{c11} calculated as in (28). In the non-saturated case, the third line and column of the LMIs (15) and (26) must be deleted, and the LMIs (16) and (27) discarded.*

6. Optimization procedures

The main objective here is to reduce the number of data transmissions on the sensor-to-controller and the controller-to-actuator channels. Let us remark that if

$$\begin{aligned} \left(\hat{y}_{k-1}-y_k\right)^\top\left(\hat{y}_{k-1}-y_k\right)\lambda_{\max}(Q_{\Delta y}) - y_k^\top y_k \lambda_{\min}(Q_y) \leq 0, \\ \left(\hat{u}_{k-1}-u_k\right)^\top\left(\hat{u}_{k-1}-u_k\right)\lambda_{\max}(Q_{\Delta u}) - u_k^\top u_k \lambda_{\min}(Q_y) \leq 0, \end{aligned}$$

then, the triggering conditions (7) and (8) do not hold, avoiding data transmission. Note that, in the worst case, that is, when the conditions become equalities, one gets:

$$\begin{aligned} \frac{\left(\hat{y}_{k-1}-y_k\right)^\top\left(\hat{y}_{k-1}-y_k\right)\lambda_{\max}(Q_{\Delta y})}{y_k^\top y_k \lambda_{\min}(Q_y)} \leq 1 \text{ and} \\ \frac{\left(\hat{u}_{k-1}-u_k\right)^\top\left(\hat{u}_{k-1}-u_k\right)\lambda_{\max}(Q_{\Delta y})}{u_k^\top u_k \lambda_{\min}(Q_u)} \leq 1, \end{aligned} \tag{31}$$

respectively. Since $\lambda_{\min}(Q_y)^{-1} = \lambda_{\max}(Q_y^{-1})$ and $\lambda_{\min}(Q_u)^{-1} = \lambda_{\max}(Q_u^{-1})$, we can rewrite (31) as

$$\begin{aligned} \frac{\left(\hat{y}_{k-1}-y_k\right)^\top\left(\hat{y}_{k-1}-y_k\right)}{y_k^\top y_k}\eta(Q_{\Delta y}, Q_y^{-1}) \leq 1 \text{ and} \\ \frac{\left(\hat{u}_{k-1}-u_k\right)^\top\left(\hat{u}_{k-1}-u_k\right)}{u_k^\top u_k}\eta(Q_{\Delta u}, Q_u^{-1}) \leq 1, \end{aligned} \tag{32}$$

respectively, with $\eta(Q_{\Delta y}, Q_y^{-1}) = \lambda_{\max}(Q_{\Delta y})\lambda_{\max}(Q_y^{-1})$ and $\eta(Q_{\Delta u}, Q_u^{-1}) = \lambda_{\max}(Q_{\Delta u})\lambda_{\max}(Q_u^{-1})$. Thus, the idea is to minimize $\eta(Q_{\Delta y}, \hat{Q}_y)$ and $\eta(Q_{\Delta u}, \hat{Q}_u)$, with $\hat{Q}_y = Q_y^{-1}$ and $\hat{Q}_u = Q_u^{-1}$, so that the minimum time required for the expressions on the left hand-side of (31) to evolve from 0 to 1 is enlarged. However, $\eta(Q_{\Delta y}, \hat{Q}_y)$, and $\eta(Q_{\Delta u}, \hat{Q}_u)$ are not convex functions and therefore it can be difficult to optimize them. Nevertheless, one can observe that the event-triggering functions depend on all the eigenvalues of $Q_{\Delta y}$, $\hat{Q}_y$, $Q_{\Delta u}$ and $\hat{Q}_u$. So, to formulate a convex objective function, we can minimize the sum of all eigenvalues of $Q_{\Delta y}$, $\hat{Q}_y$, $Q_{\Delta y}$ and $\hat{Q}_y$, which leads to the following convex optimization procedure:

$$\mathcal{O}_1 : \begin{cases} \min & \texttt{tr}(Q_{\Delta y}+\hat{Q}_y) + \texttt{tr}(Q_{\Delta u}+\hat{Q}_u), \\ \text{subject to} & \begin{cases} (15) \text{ and } (16), \\ \quad \text{or} \\ (26) \text{ and } (27). \end{cases} \end{cases} \tag{33}$$

Let us point out that the data transmission is indirectly reduced by means of the optimization procedure $\mathcal{O}_1$.

Another objective of optimization consists in considering a given region of admissible initial states $\mathcal{X}_0$ for which we can reduce the update rate on the sensor-to-controller and the controller-to-sensor channels. In this case, we should ensure that $\mathcal{X}_0$ is included in the region of attraction of the closed-loop systems, i.e. $\mathcal{X}_0 \subseteq \mathcal{R}_\mathcal{E} \subseteq \mathcal{R}_\mathcal{A}$. If $\mathcal{X}_0$ is specified as an ellipsoid $\mathcal{E}(R,1)$, defined similarly to (14), then we have that

$$\left[\begin{array}{cc} R & \star \\ \mathbf{I}_{2n} & P_i \end{array}\right] > \mathbf{0}, \text{ or equivalently} \tag{34a}$$

$$\left[\begin{array}{cc} R & \star \\ \Phi^\top & \hat{P}_i \end{array}\right] > \mathbf{0}, \tag{34b}$$

with Φ given in (22), for all $i \in \mathcal{I}[1, N]$. However, the LMI (34b) is non-convex due to the presence of the matrix W in Φ. To make it convex, we can consider the partitioning $R = \begin{bmatrix} R_{11} & \star \\ R_{21} & R_{22} \end{bmatrix}$ and $x_{c,0} = \mathbf{0}$, which allows us to dismiss the rows concerning the position of W in Φ. With that, the inequality (34b) can be rewritten as

$$\left[\begin{array}{c|c} R_{11} & \star \\ \hline Y & \hat{P}_i \\ \mathbf{I}_n & \end{array}\right] > \mathbf{0}, \tag{35}$$

for all $i \in \mathcal{I}[1, N]$. Thus, we have

$$\mathcal{O}_2 : \begin{cases} \min & \mathtt{tr}(Q_{\Delta_y} + \hat{Q}_y) + \mathtt{tr}(Q_{\Delta u} + \hat{Q}_u), \\ \text{subject to} & \begin{cases} (15), (16) \text{ and } (34a), \\ \quad \text{or} \\ (26), (27) \text{ and } (35), \end{cases} \end{cases} \tag{36}$$

with $\hat{Q}_y = Q_y^{-1}$ and $\hat{Q}_u = Q_u^{-1}$.

Although both optimization procedures aim at minimizing the data transmission, the optimization procedure $\mathcal{O}_2$ differs from the optimization procedure $\mathcal{O}_1$ by the inclusion of the restrictions (34a) and (35) to take into account a specific region of initial condition. It is important to point out that, the use of the optimization procedure $\mathcal{O}_2$ leads to deal with a classical trade-off between the size of the estimate of the basin of attraction and the transmission saving. Indeed, it results that the smaller the estimate of the basin of attraction, the greater the transmission saving.

7. Simulation results

In this section, some examples addressing both the LPV and the LTI cases, with and without saturating actuators, are explored. First, we present two examples relating to LTI systems and then a third example concerning an LPV system with saturating actuators.

Example 1 Consider the following discretized version, with sampling time $T_s = 0.05$ seconds, of the system investigated in [19].

$$\begin{aligned} x_{p,k+1} &= \begin{bmatrix} 1 & 0.05 \\ 0.1 & 0.85 \end{bmatrix} x_{p,k} + \begin{bmatrix} 0.11 \\ 0.11 \end{bmatrix} \hat{u}_k, \\ y_k &= \begin{bmatrix} -1 & 4 \end{bmatrix} x_{p,k}. \end{aligned} \tag{37}$$

Our objective here is to compare our co-design and emulation proposals with the one in [19]. The authors in [19] address the co-design event-triggered dynamic output-feedback control problem for continuous linear time-invariant (LTI) system. The two independent ETMs are based on a condition that depends on the plant output and the controller output taken at different times. The results obtained by [19] are presented in Table 1, where the initial conditions $x_{p,0} = x_{c,0} = \begin{bmatrix} 40 & -20 \end{bmatrix}^\top$ were taken to simulate the closed-loop response of the system. Observe that, in the first channel, [19] got an average sampling time that corresponds to 3 times the sampling time of the system without ETM; and, in the second channel, the average sampling time found corresponds to 3.6 times the sampling time of the system without ETM.

Table 1
Comparison of the average sampling time - Example (37).

Design method	average sampling time [sec]	
	output	control
Theorem 2 in [19]	0.15	0.18
Theorem 1	0.2303	0.25
Theorem 2	0.2303	0.375

First, to compare the co-design approach, we solve the optimization procedure $\mathcal{O}_1$ given in (33) with conditions of Theorem 2, and obtain the ETM matrices $Q_{\Delta_y} = 1.5489$, $Q_y = 0.7091$, $Q_{\Delta u} = 1.4102$, and $Q_u = 0.6456$ and the following dynamic controller matrices

$$A_c = \begin{bmatrix} 6.1903 & 3.8725 \\ -8.3910 & -5.2462 \end{bmatrix}, \; B_c = \begin{bmatrix} -17.4254 \\ 23.6933 \end{bmatrix},$$
$$C_c = \begin{bmatrix} 0.1654 & 0.1180 \end{bmatrix}, \text{ and } D_c = -1.2314.$$

By simulating the closed-loop response of the system for the same initial conditions, we got the average sampling times presented in Table 1. Note that, in the first channel, we obtained an average sampling time that corresponds to almost 5 times the sampling time of the system without ETM, and in the second channel, the average sampling time found corresponds to 7.5 times the sampling time of the system without ETM. Therefore, we increased the average sampling in 53.87% on the sensor-to-controller channel, and 108.33% on controller-to-actuator channel, with respect to [19].

Then, to compare the emulation-approach, we design the ETMs (7) and (8) for both the controller obtained in the co-design and the one obtained by [19] using the optimization procedure $\mathcal{O}_1$ given in (33) with conditions of Theorem 1. For the first case, we have found the same results, and for the second, we got the ETM matrices $Q_{\Delta_y} = 1.8588$, $Q_y = 0.2646$, $Q_{\Delta u} = 3.7788$ and $Q_u = 0.5380$. By using these matrices to simulate the closed-loop response of the system, we find the average sampling times presented in Table 1. Thus, using our controller, the sampling average in the control ETM improved 50% in relation to the controller of [19].

Example 2 Consider the following discretized version, with sampling time $T_s = 0.05$ seconds, of the system investigated in [18]

$$\begin{aligned} x_{p,k+1} &= \begin{bmatrix} 1 & 0.05 \\ -0.25 & 1 \end{bmatrix} x_{p,k} + \begin{bmatrix} 0 \\ 0.05 \end{bmatrix} \hat{u}_k, \\ y_k &= \begin{bmatrix} 1 & 0 \end{bmatrix} x_{p,k}. \end{aligned} \tag{38}$$

Our objective here is to compare our co-design approach with the one in [18], where a co-design of a dynamic output-feedback controllers and two independent ETMs for continuous linear time-invariant system with communication delays are proposed. The results obtained by [18] are showed in Table 2, where the initial states condition $x_{p,0} = \begin{bmatrix} 1 & 0.2 \end{bmatrix}^\top$ and

Table 2
Comparison of the updates rates - Example (38).

Design Method	Updates rates (%)	
	output	control
[18, Th. 2]	34.50%	38.25%
Theorem 2	30.50%	36.25%

$x_{c,0} = \mathbf{0}_{1,2}$ were taken to simulated the closed-loop response. By taking into account the procedures described in Remark 4 to deal with LTI ($\rho_k = 0$) and non-saturated system, we run the optimization procedure $\mathcal{O}_1$ given in (33) with conditions of Theorem 2, and got the ETM matrices $Q_{\Delta y} = 2.6910$, $Q_y = 0.6063$, $Q_{\Delta u} = 1.6493$, and $Q_u = 0.3716$ and the following dynamic controller matrices

$$A_c = \begin{bmatrix} 1.0819 & 0.5297 \\ -0.4837 & -0.2445 \end{bmatrix}, \; B_c = \begin{bmatrix} -5.9799 \\ 2.6499 \end{bmatrix},$$
$$C_c = \begin{bmatrix} 0.4254 & 1.1925 \end{bmatrix}, \text{ and } D_c = -2.3619.$$

For the same initial conditions, we simulated the response of the closed-loop system and got the transmission rates showed in Table 2. In this case, we reduced the update rate in 6.15% and 5.23% on the sensor-to-controller and controller-to-actuator channels, respectively, in relation to [18].

Example 3 Consider the inverted pendulum shown in Figure 2. This system has been extensively investigated in the literature (see, for example, [33, 11, 6]), but without taking into account possible variations in the system parameters. Let us then consider such variations by adding the parameter-varying ρ_k to the system model, as follows

$$x_{p,k+1} = \begin{bmatrix} 1.0018 & 0.01 \\ 0.04\rho_k + 0.36 & 1.0018 \end{bmatrix} x_{p,k} + \begin{bmatrix} -0.001 \\ 0.025\rho_k - 0.184 \end{bmatrix} \mathtt{sat}(\hat{u}_k), \quad (39)$$

with $y_k = \begin{bmatrix} 1 & 0 \end{bmatrix} x_{p,k}$, $\bar{u} = 1$ and $|\rho_k| \leq 1$. Note that, this

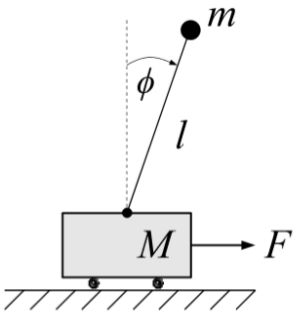

Figure 2: An inverted pendulum [33]

arbitrary variation was added just to test our approach, and, therefore, has no direct physical meaning with the continuous-time system's variables. Our objective here is to made the co-design of the dynamic controller (6) and the two ETMs (7) and (8), for two different given admissible initial conditions region $\mathcal{X}_0$, such that the number of data transmissions in both channels is as low as possible.

For the first case, let us consider a given region of admissible initial conditions $\mathcal{X}_0 = \mathcal{E}(R, 1)$ with $R_{11} = \mathtt{diag}\{76, 2\}$ derived from the partitioning of R. By using the optimization procedure $\mathcal{O}_2$ with conditions of Theorem 2, we design simultaneously the dynamic controller (6) and the two independent ETMs (7) and (8) such that the update on the sensor-to-controller and the controller-to-actuator channels are minimized. Through this, we got the ETM matrices $Q_{\Delta y} = 18.8382$, $Q_y = 0.2365$, $Q_{\Delta u} = 3.6281$, and $Q_u = 0.0516$ and the following dynamic controller matrices

$$A_{c11} = \begin{bmatrix} 2.0127 & 2.1023 \\ -0.3230 & -0.3377 \end{bmatrix}, A_{c12} = \begin{bmatrix} 0.9254 & -4.9222 \\ -0.1469 & 0.7998 \end{bmatrix},$$
$$A_{c22} = \begin{bmatrix} 0.0834 & -10.4533 \\ -0.0125 & 1.6824 \end{bmatrix}, \; B_{c11} = \begin{bmatrix} -26.0948 \\ 4.1866 \end{bmatrix},$$
$$B_{c12} = \begin{bmatrix} -22.1621 \\ 3.5556 \end{bmatrix}, B_{c22} = \begin{bmatrix} -16.4072 \\ 2.6323 \end{bmatrix}, E_{c1} = \begin{bmatrix} 0.3900 \\ -0.0626 \end{bmatrix},$$
$$E_{c2} = \begin{bmatrix} 2.5333 \\ -0.4064 \end{bmatrix}, \; C_{c1} = \begin{bmatrix} -0.2975 \\ -2.1999 \end{bmatrix}^\top, \; C_{c2} = \begin{bmatrix} -0.1745 \\ -1.4513 \end{bmatrix}^\top,$$
$$D_{c1} = 6.8209, \text{ and } D_{c2} = 7.8238.$$

Figure 3 shows the projection (–) and the cut (–), on the plane defined by the plant states, of the $\mathcal{R}_\mathcal{E}$ obtained, $\mathcal{X}_0$ (–), and also the projections of some convergent (--) and some divergent trajectories (--) starting from the points marked with ∘ and ∗, respectively. Notice that, as required, $\mathcal{R}_\mathcal{E}$ contains $\mathcal{X}_0$, i.e. $\mathcal{X}_0 \subset \mathcal{R}_\mathcal{E}$. In particular, for the convergent trajectory (--) starting in the initial condition $x_0 = \begin{bmatrix} -0.1480 & -0.4735 & 0 & 0 \end{bmatrix}^\top$ marked with '•', we plot in the Figure 4 the states, the control input, the events of the sensor and the controller, and the parameter-varying as a function of the sampling instants. In the inter-events graph, the events that occur asynchronously in the sensor and in the controller are represented by '∘' and '∘', respectively, and synchronous by '∘'. Thus, we can see the asymptotic stability of the system despite the saturation in the first instants of the simulation. For this case, the update rate between the sensor and controller and between the controller and actuator was 50.33% and 43%, respectively, thus, saving a significant amount of samples to be transmitted. However, the inclusion of $\mathcal{X}_0$ yielded an ETM behavior that appears to have some periodicity despite the asynchronous updates of sensor and control ETMs. Moreover, the asynchronous ETMs save transmissions because only one ETM is active over the network.

Then, for the second case, we carried out the co-design for a region of admissible initial conditions less stringent, given by $\mathcal{X}_0 = \mathcal{E}(R, 1)$ with $R_{11} = \mathtt{diag}\{26.60, 0.70\}$ derived from the partitioning of R. For this case, we obtained the ETM matrices $Q_{\Delta y} = 29.5663$, $Q_y = 0.0881$, $Q_{\Delta u} = 5.8971$, and $Q_u = 0.0221$ and the dynamic controller matri-

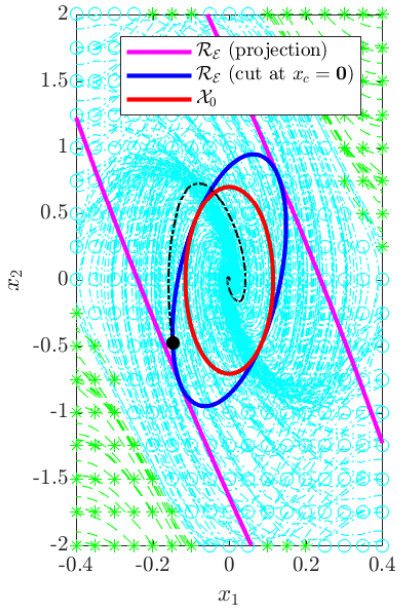

Figure 3: $\mathcal{R}_\mathcal{E}$ and $\mathcal{X}_0 = \mathcal{E}(P, 1)$ with $R_{11} = \texttt{diag}\{76, 2\}$.

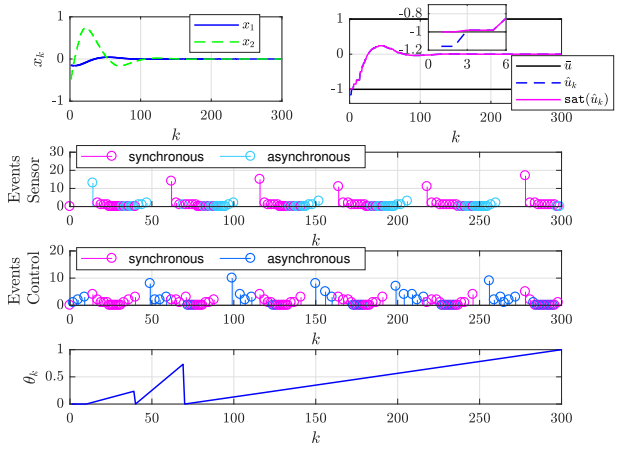

Figure 4: The closed-loop response of system (39) - $\mathcal{X}_0 = \mathcal{E}(P, 1)$ with $R_{11} = \texttt{diag}\{76, 2\}$.

ces

$$A_{c11} = \begin{bmatrix} 5.2362 & 20.9969 \\ -0.8710 & -3.4869 \end{bmatrix}, \; A_{c12} = \begin{bmatrix} 2.9999 & 7.3585 \\ -0.5051 & -1.2549 \end{bmatrix},$$

$$A_{c22} = \begin{bmatrix} -0.0841 & -11.4126 \\ 0.0137 & 1.9028 \end{bmatrix}, \; B_{c11} = \begin{bmatrix} -6.4201 \\ 1.0716 \end{bmatrix},$$

$$B_{c12} = \begin{bmatrix} -4.9392 \\ 0.8246 \end{bmatrix}, \; B_{c22} = \begin{bmatrix} -2.7266 \\ 0.4550 \end{bmatrix}, \; E_{c1} = \begin{bmatrix} 3.7979 \\ -0.6337 \end{bmatrix},$$

$$E_{c2} = \begin{bmatrix} 4.3923 \\ -0.7330 \end{bmatrix}, \; C_{c1} = \begin{bmatrix} 1.7658 \\ 9.7753 \end{bmatrix}^\top, \; C_{c2} = \begin{bmatrix} -0.0633 \\ -1.2096 \end{bmatrix}^\top,$$

$D_{c1} = 5.5867$, and $D_{c2} = 6.2479$.

Figure 5 presents the projection and the cut, on the plane defined by the plant states, of the $\mathcal{R}_\mathcal{E}$ obtained. For the convergent trajectory (--) starting in the initial condition $x_0 = \begin{bmatrix} -0.2117 & -0.3245 & 0 & 0 \end{bmatrix}^\top$ marked with "•", we simulated the closed-loop response of the system, and the results can be seen in the Figure 6. In this case, the update rates between the sensor and controller and between the controller and actuator found were 67.33% and 59.67%, respectively. Therefore, in relation to the update rate, there was a slight worse performance than the more restrictive (on the plane defined by the plant states) $\mathcal{X}_0$ specification. The ETMs seem to present a more pronounced periodic behavior in this case, which may be connected to the higher transmission rate achieved due to the inclusion of a larger region of initial condition considered here (w.r.t. that one in the previous case). Another effect of including a larger $\mathcal{X}_0$ is the reduction on the asynchronous transmission, supporting the hypothesis of the bigger the region of initial conditions, the smaller the transmissions saving.

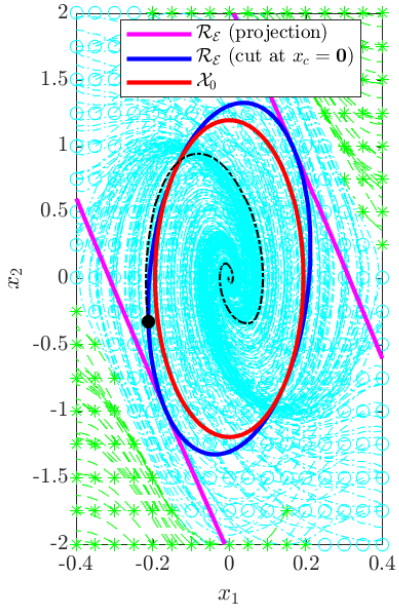

Figure 5: $\mathcal{R}_\mathcal{E}$ and $\mathcal{X}_0 = \mathcal{E}(R, 1)$ with $R_{11} = \texttt{diag}\{26.60, 0.70\}$.

The inverted pendulum is also investigated in [6], where the design of event-triggering static and dynamic state stabilizing controllers for discrete-time linear systems with saturating actuators is addressed. The number of updates obtained by [6] are showed in Table 3, where the initial conditions $x_{p,0} = \begin{bmatrix} 0.2 & 0.8 \end{bmatrix}^\top$ and $x_{c,0} = \begin{bmatrix} 0 & 0 \end{bmatrix}^\top$ were taken to simulate the closed-loop response of the system. Observe that since [6] does not consider a communication network between the controller and actuator channel, then the system updates the control at all sampling times.

As the authors in [6] explore the LTI case with saturation, to compare our approach with theirs, we fix $\rho_k = 0$, and set $C = \mathbf{I}_2$. Also, we consider a region of admissible initial conditions $\mathcal{X}_0 = \mathcal{E}(R, 1)$ with $R_{11} = \begin{bmatrix} 11.9987 & 0.2318 \\ 0.2318 & 0.5873 \end{bmatrix}$, which is contained in the region of attraction estimated by [6]. Thus, for the co-design, we run the optimization proce-

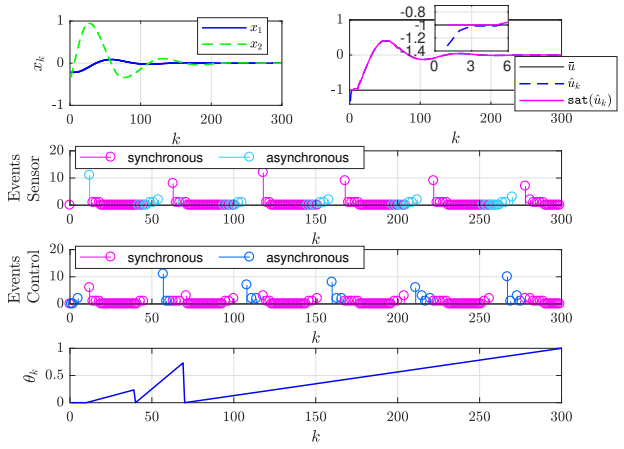

Figure 6: The closed-loop response of system (39) - $\mathcal{X}_0 = \mathcal{E}(R, 1)$ with $R_{11} = \mathtt{diag}\{26.60, 0.70\}$.

Table 3
Comparison of the number of samplings - Example (39).

Design method	update	
	output	control
Theorem 3.1 in [6]	67	1000
Theorem 4.1 in [6]	70	1000
Theorem 2	85	232

dure $\mathcal{O}_2$ with conditions of Theorem 2, and got the following ETM matrices

$$Q_{\Delta y} = \begin{bmatrix} 1.2955 & 0.9134 \\ 0.9134 & 0.6441 \end{bmatrix}, \; Q_y = \begin{bmatrix} 0.0758 & 0.0106 \\ 0.0106 & 0.0425 \end{bmatrix},$$
$$Q_{\Delta u} = 1.5369, \text{ and } Q_u = 0.0261,$$

and the following dynamic controller matrices

$$A_c = \begin{bmatrix} -6.3069 & -29.0632 \\ 1.5869 & 7.3118 \end{bmatrix}, \; B_c = \begin{bmatrix} -0.0264 & -0.0186 \\ 0.0067 & 0.0047 \end{bmatrix},$$
$$E_c = \begin{bmatrix} -0.1133 \\ 0.0288 \end{bmatrix}, \; C_c = \begin{bmatrix} -6.6853 \\ -3.1688 \end{bmatrix}^\top, \text{ and } D_c = \begin{bmatrix} 1.3583 \\ 0.9577 \end{bmatrix}^\top.$$

For the same initial condition, we simulate the closed-loop response of the system, and found the updates rates showed in Table 3. Although, in the first channel, the update rates obtained by [6] with Theorem 3.1 and Theorem 4.1 are 21.18% and 17.65% smaller than ours, respectively, in the second channel, they are in both cases 331.03% higher than ours.

8. Conclusion

In this paper, the dynamic event-triggered control problem was investigated for a discrete-time LPV system subject to actuator saturation. The measured output and the control input are transmitted based on two independent event-triggering schemes. Both emulation-based approach and co-design of the event-generators parameters and the controller matrices were proposed. The convex conditions in form of linear matrix inequalities (LMIs) ensured the regional asymptotic stability of the closed-loop system for every initial condition belonging to the estimated attraction region. Some optimization procedures were also formulated allowing the minimization of the data transmission on the sensor-to-control and control-to-actuator channels. As future work, it would be interesting to study if the two event-triggering mechanisms (7) and (8) could be dependent (that is, each ETM could use information from the other transmitted signal).

References

[1] Abdelrahim, M., Postoyan, R., Daafouz, J., Nešić, D., Heemels, M., 2018. Co-design of output feedback laws and event-triggering conditions for the $\mathcal{L}_2$-stabilization of linear systems. Automatica 87, 337–344.

[2] Braga, M.F., Morais, C.F., Tognetti, E.S., Oliveira, R., P.L.D.Peres, 2015. Discretization and event triggered digital output feedback control of LPV systems. Systems & Control Letters 86, 54–65.

[3] Briat, C., 2014. Linear Parameter-Varying and Time-Delay Systems: Analysis, Observation, Filtering & Control. Spring, Berlin.

[4] de Souza, C., Tarbouriech, S., Castelan, E., Leite, V., 2020a. Event-triggered dynamic output-feedback controller for discrete-time LPV systems with constraints, in: 24th International Symposium on Mathematical Theory of Networks and Systems, pp. 1–6. Accepted.

[5] de Souza, C., Tarbouriech, S., Leite, V., Castelan, E., 2020b. Co-design of an event-triggered dynamic output feedback controller for discrete-time LPV systems with constraints. Journal of The Franklin Institute Submitted.

[6] Ding, S., Xie, X., Liu, Y., 2020. Event-triggered static/dynamic feedback control for discrete-time linear systems. Information Sciences .

[7] Eqtami, A., Dimarogonas, D.V., Kyriakopoulos, K.J., 2010. Event-triggered control for discrete-time systems, in: Proceedings of the 2010 american control conference, IEEE. pp. 4719–4724.

[8] Ge, X., Han, Q.L., Ding, L., Wang, Y.L., Zhang, X.M., 2020. Dynamic event-triggered distributed coordination control and its applications: A survey of trends and techniques. IEEE Transactions on Systems, Man, and Cybernetics: Systems .

[9] Golabi, A., Meskin, N., Tóth, R., Mohammadpour, J., Donkers, T., 2016. Event-triggered control for discrete-time linear parameter-varying systems, in: 2016 American Control Conference (ACC), IEEE. pp. 3680–3685.

[10] Golabi, A., Meskin, N., Tóth, R., Mohammadpour, J., Donkers, T., Davoodi, M., 2017. Event-triggered constant reference tracking control for discrete-time LPV systems with application to a laboratory tank system. IET Control Theory & Applications 11, 2680–2687.

[11] Groff, L., Moreira, L., Gomes da Silva, J., 2016. Event-triggered control co-design for discrete-time systems subject to actuator saturation, in: 2016 IEEE Conference on Computer Aided Control System Design (CACSD), IEEE. pp. 1452–1457.

[12] Heemels, W., Donkers, M., Teel, A., 2012a. Periodic event-triggered control for linear systems. IEEE Transactions on Automatic Control 58, 847–861.

[13] Heemels, W., Johansson, K.H., Tabuada, P., 2012b. An introduction to event-triggered and self-triggered control, in: 2012 IEEE 51st IEEE Conference on Decision and Control (CDC), pp. 3270–3285.

[14] Hespanha, J.P., Naghshtabrizi, P., Xu, Y., 2007. A survey of recent results in networked control systems. Proceedings of the IEEE 95, 138–162.

[15] Jungers, M., Castelan, E.B., 2011. Gain-scheduled output control design for a class of discrete-time nonlinear systems with saturating actuators. Systems & Control Letters 60, 169–173.

[16] Li, S., Sauter, D., Xu, B., 2015. Co-design of event-triggered $\mathcal{H}_\infty$ control for discrete-time linear parameter-varying systems with network-induced delays. Journal of the Franklin Institute 352, 1867–1892.

[17] Li, S., Xu, B., 2013. Event-triggered control for discrete-time uncer-

tain linear parameter-varying systems, in: Proceedings of the 32nd Chinese Control Conference, IEEE. pp. 273–278.
[18] Liu, D., Yang, G.H., 2018. Robust event-triggered control for networked control systems. Information Sciences 459, 186–197.
[19] Ma, D., Han, J., Zhang, D., Liu, Y., 2015. Co-design of event generator and dynamic output feedback controller for LTI systems. Mathematical Problems in Engineering 2015.
[20] Moreira, L.G., Groff, L.B., Gomes da Silva Jr, J., Tarbouriech, S., 2019. PI event-triggered control under saturating actuators. International Journal of Control 92, 1634–1644.
[21] Peng, C., Yang, T.C., 2013. Event-triggered communication and $\mathcal{H}_\infty$ control co-design for networked control systems. Automatica 49, 1326–1332.
[22] Postoyan, R., Tabuada, P., Nešić, D., Anta, A., 2014. A framework for the event-triggered stabilization of nonlinear systems. IEEE Transactions on Automatic Control 60, 982–996.
[23] Ramezanifar, A., Mohammadpour, J., Grigoriadis, K.M., 2015. Sampled-data filtering for linear parameter varying systems. International Journal of Systems Science 46, 474–487.
[24] Scherer, C., Gahinet, P., Chilali, M., 1997. Multiobjective output-feedback control via LMI optimization. IEEE Transactions on automatic control 42, 896–911.
[25] de Souza, C., Leite, V.J.S., Tarbouriech, S., Castelan, E.B., 2020. Emulation-based dynamic output-feedback control of saturating discrete-time LPV systems. IEEE Control Systems Letters 5, 1549–1554.
[26] Tabuada, P., 2007. Event-triggered real-time scheduling of stabilizing control tasks. IEEE Transactions on Automatic Control 52, 1680–1685.
[27] Tanwani, A., Prieur, C., Fiacchini, M., 2016. Observer-based feedback stabilization of linear systems with event-triggered sampling and dynamic quantization. Systems & Control Letters 94, 46–56.
[28] Tarbouriech, S., Garcia, G., Gomes da Silva Jr., J.M., Queinnec, I., 2011. Stability And Stabilization Of Linear Systems With Saturating Actuators. (Springer.
[29] Tarbouriech, S., Seuret, A., Gomes da Silva Jr, J.M., Sbarbaro, D., 2016. Observer-based event-triggered control co-design for linear systems. IET Control Theory & Applications 10, 2466–2473.
[30] Toth, R., Heuberger, P.S.C., Van den Hof, P.M.J., 2010. Discretisation of linear parameter-varying state-space representations. IET control theory & applications 4, 2082–2096.
[31] Verdult, V., 2002. Nonlinear system identification: State-space approach. Ph.D. thesis. Faculty of Applied Physics,University of Twente. Enschede, The Netherlands.
[32] Wu, W., Reimann, S., Görges, D., Liu, S., 2016. Event-triggered control for discrete-time linear systems subject to bounded disturbance. International Journal of Robust and Nonlinear Control 26, 1902–1918.
[33] Wu, W., Reimann, S., Liu, S., 2014. Event-triggered control for linear systems subject to actuator saturation. IFAC Proceedings Volumes 47, 9492–9497.
[34] Xie, X., Li, S., Xu, B., 2018. Output-based event-triggered control for networked control systems: tradeoffs between resource utilisation and robustness. IET Control Theory & Applications 12, 2138–2147.
[35] Yue, D., Tian, E., Han, Q.L., 2012. A delay system method for designing event-triggered controllers of networked control systems. IEEE Transactions on Automatic Control 58, 475–481.
[36] Zhang, P., Liu, T., Jiang, Z.P., 2017. Input-to-state stabilization of nonlinear discrete-time systems with event-triggered controllers. Systems & Control Letters 103, 16–22.
[37] Zhang, X.M., Han, Q.L., 2014. Event-triggered dynamic output feedback control for networked control systems. IET Control Theory & Applications 8, 226–234.
[38] Zuo, Z., Li, Q., Li, H., Wang, Y., 2016. Co-design of event-triggered control for discrete-time systems with actuator saturation, in: 2016 12th World Congress on Intelligent Control and Automation (WCICA), IEEE. pp. 170–175.